Applied Surface Science 214 (2003) 304–311

A liquid aluminum corrosion resistance surface on steel substrate

Wang Deqing[a,*], Shi Ziyuan[a], Zou Longjiang[b]

[a]*Department of Materials Science and Engineering, Dalian Railway Institute, 794 Huanghe Road, Dalian, Liaoning 116028, PR China*

[b]*Dalian University of Technology, Liaoning 116028, PR China*

Received 20 July 2002; received in revised form 19 November 2002; accepted 9 March 2003

Abstract

The process of hot dipping pure aluminum on a steel substrate followed by oxidation was studied to form a surface layer of aluminum oxide resistant to the corrosion of aluminum melt. The thickness of the pure aluminum layer on the steel substrate is reduced with the increase in temperature and time in initial aluminizing, and the thickness of the aluminum layer does not increase with time at given temperature when identical temperature and complete wetting occur between liquid aluminum and the substrate surface. The thickness of the Fe–Al intermetallic layer on the steel base is increased with increasing bath temperature and time. Based on the experimental data and the mathematics model developed by the study, a maximum exists in the thickness of the Fe–Al intermetallic at certain dipping temperature. X-ray diffraction (XRD) and energy dispersive X-ray (EDX) analysis reveals that the top portion of the steel substrate is composed of a thin layer of α-Al_2O_3, followed by a thinner layer of $FeAl_3$, and then a much thicker one of Fe_2Al_5 on the steel base side. In addition, there is a carbon enrichment zone in diffusion front. The aluminum oxide surface formed on the steel substrate is in perfect condition after corrosion test in liquid aluminum at 750 °C for 240 h, showing extremely good resistance to aluminum melt corrosion.

Keywords: Aluminizing; Diffusion; Intermetallic compounds; Corrosion protection

1. Introduction

Aluminum melt is extremely corrosive and can react with nearly all metals and metal oxides due to its chemical reactivity. The crucibles used for processing liquid aluminum at present are mainly of two kinds. One is made of ceramics such as graphite or aluminum oxide, and another is iron base metallic ones made of low carbon steels and alloy cast irons with coating guard on their inside wall. Although the ceramic crucibles are excellent in corrosion resistance to liquid aluminum, they are subjected to rapid strength degradation after repeated heating and cooling cycles. Besides, it is hard to make a ceramic crucible with large capacity due to its low strength. The disadvantage of iron base crucibles is that when the coating guard falls off, the exposed iron substrate will dissolve into liquid aluminum, which results in rapid corrosion of crucible and contamination of the aluminum melt. The best way to protect metallic crucibles against aluminum melt corrosion is to form a layer of lasting, fast and stable oxide on crucible surface.

Hot dip aluminizing [1,2] has been successfully used to form a thin layer of aluminum on the surface of steel substrate for improving the service property of

* Corresponding author. Tel.: +86-411-3683348; fax: +86-411-4606139.
E-mail address: wdeqing@online.ln.cn (W. Deqing).

0169-4332/03/$ – see front matter
doi:10.1016/S0169-4332(03)00505-1

steels, especially in corrosion resistance applications [3,4]. In the process, when wetting the surface of steel substrate, Al diffuses into steel to form Fe–Al intermetallics according to Fe–Al binary phase diagram [5]. Due to its high micro-hardness (HV 750–850) and high aluminum content (49–59 wt.%), the surface layer of the Fe–Al intermetallics has extremely good resistance to wear and thermal erosion at temperatures between 450 and 980 °C [6,7]. By oxidation of the aluminum layer on the surface of steel substrate, the steel base will be protected by a layer of aluminum oxide that has high melting point, great hardness, thermodynamic stability and poor wetting with aluminum melt [8]. The wetting angle between alumina and aluminum melt below 900 °C is 138°, which is the largest among common metal oxides [9].

The present work aims to form an anti-corrosion surface on steel for processing liquid aluminum by aluminizing and oxidation. The hot dip and oxidation processes and the microstructure changes of the steel substrate are also investigated.

2. Experimental procedure

2.1. Materials

The steel substrate used was Φ 16 mm bar in annealed condition, its chemical composition is listed in Table 1. The samples to be aluminized were cut from the bar with dimensions of diameter = 16 mm and thickness = 6 mm. High purity aluminum (>99.9%) was used for the dipping bath.

2.2. Aluminizing

Aluminum was melted in graphite crucible in a resistance furnace, and the melt was maintained at different dipping temperatures, 690, 710 and 730 °C. The steel substrate without preheating after degreasing, activation and drying was immerged into the liquid aluminum for different holding times. Then, the sample was taken out from the melt and cooled in air to room temperature.

Table 1
Chemical compositions of the steel substrate

Elements	Composition (wt.%)
C	0.44
Mn	0.30
Si	0.25
S	0.019
P	0.016
Fe	Balance

2.3. Oxidation

The aluminized sample was placed in a resistance furnace where it was heated in air to a temperature of 550 °C over a 1-h heat-up period, and then maintained at 550 °C for 1 h. Subsequently, the furnace temperature was raised to 650 °C and then held at 650 °C for 1 h. These heating steps permitted the formation of a certain thickness of oxide layer on the aluminized sample surfaces sufficient per se to prevent aluminum from dripping, and thus to maintain the smoothness and uniformity of the surface layer. At this point, the furnace temperature was increased to 850 °C over a 1-h period, and was maintained there for 1 h. After the oxidation, the sample was cooled inside the furnace.

2.4. Corrosion test

Controlled corrosion test was conducted in pure aluminum bath at 750 °C for 240 h by immerging the steel substrate and the sample after aluminizing and oxidation treatments.

2.5. Analysis of samples

For microstructure observation and analysis, the specimens were carefully mounted, ground, and polished to protect the edges. The specimens were etched with a 3% nital solution to reveal the coating layers. The thickness of the layers was measured at least five times at different places on the section.

Microstructure observation and analysis and chemical composition determination were performed by optical microscopy and scanning electron microscopy (SEM) with energy dispersive X-ray facility (EDX). The EDX facility was calibrated by using SiC and TiC for quantitative determination of carbon. X-ray diffractometry (XRD) analysis in 2θ range from 20 to 120° using Cu Kα radiation was conducted to determine phase structures of the samples after aluminizing and oxidation. Micro-hardness of the

aluminized samples was also measured with a Vickers micro-hardometer.

3. Results and discussion

3.1. Microstructure changes

The cross-section of the sample after hot dipping in pure aluminum melt at 710 °C for 120 min shows the appearance of an intermetallic layer (440 μm on average) covered with an aluminum top coat layer (40 μm), both formed on the steel substrate composed of pearlite and ferrite, as illustrated in Fig. 1. The tongue-shaped Fe–Al intermetallics grow preferentially in length towards the steel substrate and are oriented perpendicular to the diffusion front, which leads to the formation of a serrated interface between the steel/diffusion layers. In the intermetallic zone there are numerous black spots, the cavities formed during aluminizing.

Fig. 2 shows the microstructure of the oxidized sample. The recorded diffraction pattern from an X-ray diffractometer using filtered Cu Kα radiation indicates that the phase on the surface of the steel substrate is α-Al_2O_3. Comparing with Fig. 1, it can be seen that the thickness of the surface layer after oxidation treatment has been greatly reduced due to the diffusion of aluminum into steel base, and the black cavities become larger and connected. However, a noticeable phenomenon is that very little increase in the thickness of the intermetallic layer has been detected after the oxidation treatment. Moreover, the ragged diffusion front in Fig. 1 flattens out, and a wavy and bright triple-layer-zone (70 μm) appears at the intermetallics/steel substrate interface. The total thickness of the intermetallics and the bright zone averages 460 μm. From the measurement, it is obvious that the bright zone is a diffusion product and will be discussed later.

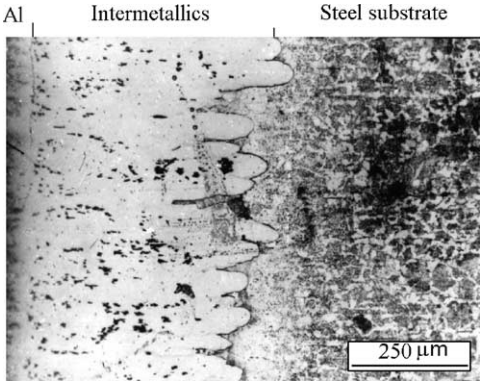

Fig. 1. Microstructure of the aluminized sample.

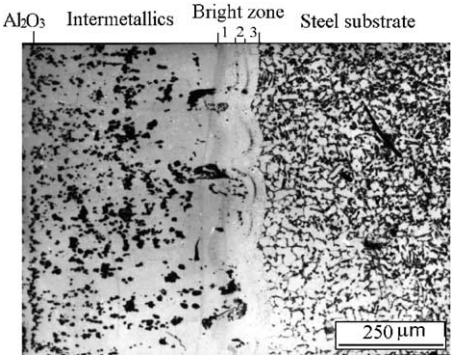

Fig. 2. Microstructure of the aluminized sample after oxidation.

Fig. 3 shows the microstructure of the sample after corrosion test in liquid aluminum. One thing differentiates from Fig. 2 is that the bright and wide triple-layer-zone before the corrosion test has combined into a bright and narrow zone (40 μm). The thickness of the intermetallic layer and the bright zone remains the same as that before the corrosion test.

3.2. Thickness of the aluminum and intermetallic layers

Fig. 4 illustrates the thickness of the pure aluminum layer on the steel base at different aluminizing

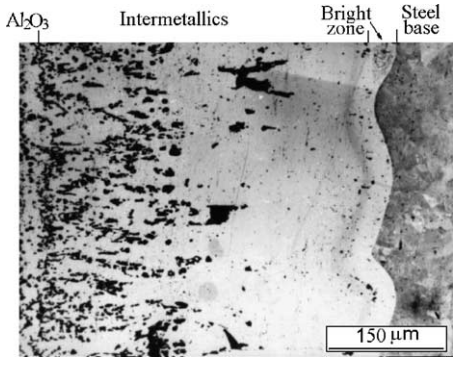

Fig. 3. Microstructure of the sample after corrosion test in liquid aluminum.

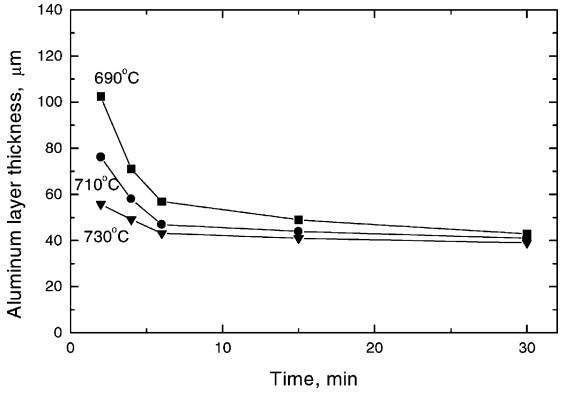

Fig. 4. Effect of dipping temperature and time on the thickness of pure aluminum layer.

temperatures and varying dipping time. At each dipping temperature, the thickness of the pure aluminum layer on the steel substrate is reduced with the increase in dipping time. When immerging time is kept constant, the thickness of the pure aluminum layer on the steel base is also decreased as the aluminizing temperature increases. However, the effects of dipping temperature and time on the thickness of the pure aluminum layer becomes insignificant when dipping time reaches 30 min, there is only about 6 μm difference in thickness for the aluminum layers at this point.

On the contrary, the thickness of the intermetallic layer in the steel substrate increases with increasing dipping temperature and time, as shown in Fig. 5.

As revealed in Fig. 4, the higher the melt temperature, and the longer the dipping time, the thinner is the

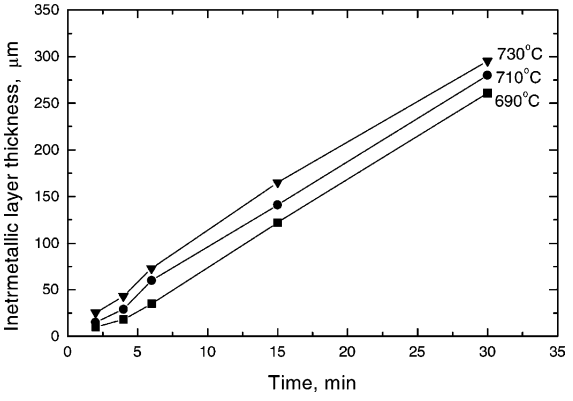

Fig. 5. Effect of dipping temperature and time on the thickness of intermetallic layer.

pure aluminum layer on the surface of the steel substrate produced. The contribution of the dipping time to the pure aluminum layer thickness results from its effect on the temperature difference between the melt and the un-preheated substrate surface. Smaller temperature difference brings a smaller viscosity difference between the block melt and the liquid around the sample surface, resulting in a thinner layer of pure aluminum on the steel substrate. The effect of immersion temperature on the pure aluminum layer thickness is that the viscosity of the aluminum melt is solely dominated by temperature. The higher the temperature, the thinner is the pure aluminum layer obtained. However, the aluminum layer will stop thickening with time at a given temperature when identical temperature and complete wetting occur between liquid aluminum and the substrate surface.

The thickness of the intermetallic layer is increased with the increase in hot dipping temperature and time. As the formation of Fe–Al intermetallics requires aluminum atoms to diffuse into the steel substrate, the rise in temperature and time favors the diffusion process to form Fe–Al intermetallics. However, when the concentration gradient of Al, or driving force for aluminum diffusion in the Fe–Al intermetallic layer becomes small enough at certain temperature according to Fe–Al binary phase diagram where Al concentration becomes less and less to Fe side, the diffusion of Al into Fe–Al intermetallics/steel substrate is difficult to continue due to the obstruction of carbon enrichment in diffusion front. Then a dynamic equilibrium of the diffusion process is reached, and the thickness of the Fe–Al intermetallics is kept constant. If dissolution of the intermetallics appears on liquid aluminum side, the thickness of the Fe–Al intermetallic layer on equilibrium at the temperature will be maintained by a forward movement of the diffusion front to compensate the thickness loss.

Being controlled by the diffusion of aluminum into iron for the formation process of the intermetallic layer, it is of practical importance to describe the relationship between the thickness of the intermetallic layer and dipping time. On the supposition that the iron dissolution into aluminum melt is negligible, the growth of the Fe–Al intermetallic phases is controlled merely by the diffusion of aluminum atoms in the intermetallic layer, and no abrupt change of aluminum concentration occurs in the layer, the change of

aluminum content c with dipping time t on equilibrium diffusion at given temperature complies with Nerst–Brummer equation [10] which is expressed as

$$\frac{dc}{dt} = -\frac{KF}{V}(c - c_m) \quad (1)$$

where K is transfer rate of aluminum atom in the Fe–Al intermetallic layer, F and V denote sample surface area and volume, and c_m is the equilibrium concentration of aluminum in the intermetallic layer.

Taken $c_{t=0} = 0$, the integral solution for Eq. (1) is

$$c = c_m\left[1 - \exp\left(-\frac{KF}{V}t\right)\right] \quad (2)$$

The aluminum concentration can also be defined as

$$c = \frac{\rho_e \varphi \cdot x}{V} \quad (3)$$

where ρ_e and φ are the equilibrium density and volume percentage of aluminum in Fe–Al intermetallic layer, and x is the thickness of the intermetallic layer.

Substitute the left and right c in Eq. (1) with Eqs. (1) and (2), respectively, we have

$$\frac{dx}{dt} = A\exp(-bt) \quad (4)$$

where

$$A = \frac{KF}{\rho \cdot \varphi}c_m \quad \text{and} \quad b = \frac{KF}{V}$$

Thus, the relationship of the Al–Fe intermetallic layer thickness as a function of time is obtained as following:

$$x = a[1 - \exp(-bt)] \quad (5)$$

where

$$a = \frac{b}{A_0}$$

Table 2 presents the thickness of the Fe–Al intermetallic layer with different dipping time at 710 °C. Using Eq. (5) for curve fitting of the experimental data in Table 4, a curve is sketched in Fig. 6 where the mathematical expression is

$$x = 448[1 - \exp(-0.03242t)] \ (\mu m) \quad (6)$$

Eq. (6) indicates that the maximum thickness of the Fe–Al intermetallic layer at 710 °C is 448 μm when time comes to infinity. In fact, this study shows that only very tiny increase in the thickness of Fe–Al intermetallic layer is detected when dipping time is over 100 min. For the same reason, the thermal cycles of the oxidation treatment and the corrosion test have hardly any effect on the thickness of the intermetallic layer formed during aluminizing on the steel substrate.

Table 2
Thickness of Fe–Al intermetallic layer with different dipping time at 710 °C

Time (min)	Thickness (μm)
2	15
4	29
6	60
15	141
30	280
60	380
100	422
120	431

3.3. Formation process of the Fe–Al intermetallics

By X-ray diffractometry (Fig. 7) together with EDX point analysis, two zones of the Fe–Al intermetallic layer have been identified. The first zone beneath the surface coating of pure aluminum is very thin and contains about 39 wt.% Fe, which is corresponding to the composition of $FeAl_3$ phase. The second zone covers the rest of the layer with the iron content of 47–51 wt.% Fe which corresponds to Fe_2Al_5.

Fig. 8 shows the SEM–EDX line profiles of element Fe, Al and C distributions across the coating layer on

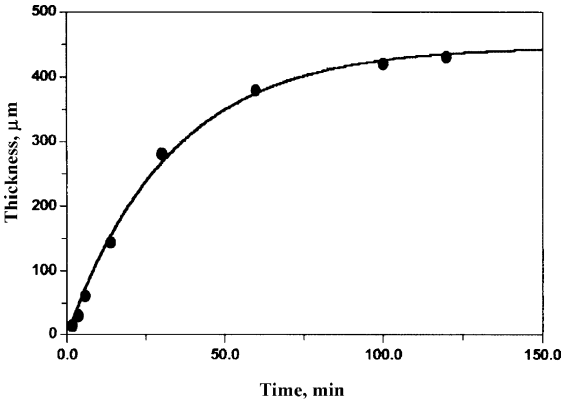

Fig. 6. Thickness of the Fe–Al intermetallic layer vs. time.

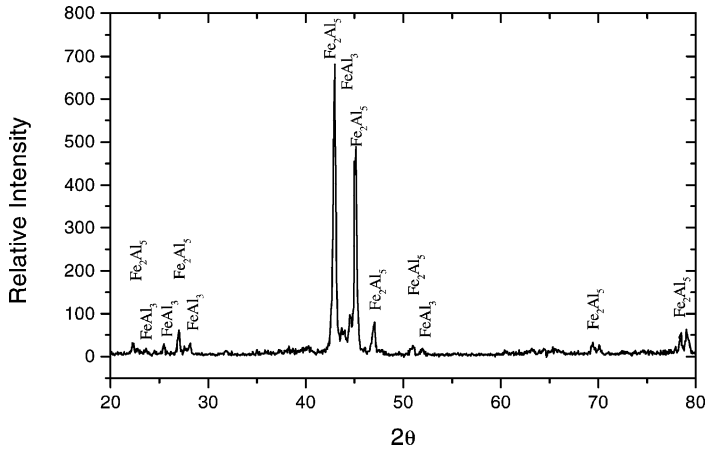

Fig. 7. X-ray diffraction pattern of the Fe–Al intermetallics.

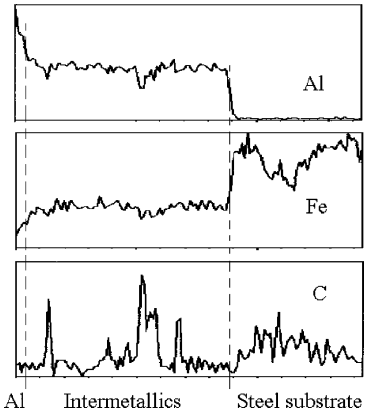

Fig. 8. SEM–EDX line profiles of element distribution in the steel substrate after aluminizing.

the steel substrate after aluminizing. A higher carbon concentration area at the diffusion front on steel substrate side was found. The peaks for carbon distribution in the intermetallic zone are caused by silicon carbide particles trapped in voids during polishing.

A considerable number of points had also been analyzed with EDX to study the carbon distribution across the Fe–Al intermetallics/steel substrate interface for the samples after oxidation treatment and corrosion test. The data from the EDX analysis are reported in Table 3, indicating a higher carbon content in the bright triple-layer-zone (Fig. 2). Even though the triple-layer-zone has merged into a narrow one (Fig. 3) after corrosion test, the carbon concentration in the zone is still larger than that in the steel substrate.

Table 3
Results of micro-hardness and EDX quantitative analysis

Sample	Position	Composition (wt.%)			Hardness (HV_{50})
		Al	Fe	C	
After aluminizing	Surface	99.87	0.13	–	37–40
	Intermetallics	68.21	31.57	0.22	784–821
After oxidation treatment	Intermetallic side	63.21	35.57	0.32	677–696
	Bright triple-layer-zone				
	Layer 1	6.42	93.03	0.55	407–438
	Layer 2	2.14	97.27	0.62	386–432
	Layer 3	0.04	99.46	0.50	374–396
	Steel substrate side	0.03	99.50	0.47	131–145
After corrosion test	Intermetallic side	48.08	50.87	0.36	362–383
	Bright zone	6.34	93.39	0.57	343–365
	Steel substrate side	0.04	99.71	0.45	115–126

Based on the growth model of Fe–Al intermetallic layer during hot dipping aluminum on low carbon steel substrate in pure aluminum melt [11], θ-$FeAl_3$ is formed first in Fe–Al interface when aluminum wets the steel surface and diffuses into steel substrate. As the diffusion rate of Al in ferrite is relatively large [12], the thickness of $FeAl_3$ layer increases with the diffusion progress. Meanwhile, tiny nucleus of η-Fe_2Al_5 phase emerges on $FeAl_3$ surface due to composition undulation, and forms η-Fe_2Al_5 phase upon reaching nucleation criteria. The crystal lattice of Fe_2Al_5 is orthorhombic, and its maximum atom concentration is only 70%. It is the 30% of voids along the *C* axis that makes Al diffuse much more rapidly into the diffusion front. Therefore, Fe_2Al_5 phase favors a rapid influx of aluminum atoms to the growth front of its crystals, resulting in a serrated interface as shown in Fig. 1. As the diffusion coefficient of iron atoms in Fe_2Al_5 phase above 700 °C is 10 times higher than that in $FeAl_3$ [13], the counter diffusion of iron atoms through Fe_2Al_5 brings the transformation of $FeAl_3$ into Fe_2Al_5, resulting in the reduction of the thickness of $FeAl_3$ phase. Consequently, the Fe–Al intermetallic layer consists mainly of the crystals of Fe_2Al_5, as shown in recorded X-ray diffraction pattern in Fig. 7, which is in good accordance with the results of EDX quantitative analysis.

In aluminizing, Al also reacts with cementite according to the following reactions:

$$Fe_3C + 9Al \rightarrow 3FeAl_3 + C \quad (7)$$

$$2Fe_3C + 15Al \rightarrow 3Fe_2Al_5 + 2C \quad (8)$$

where Al reduces carbon from cementite and combines with iron to form Fe–Al intermetallics. The carbon reduced from cementite does not react with aluminum to form Al_4C_3 under 1000 °C [14], it can react with oxygen in aluminum melt, form CO or CO_2 and then release from aluminum bath. As the oxygen content is very low in pure liquid aluminum, the carbon reduced is pushed to the diffusion front where a carbon enrichment zone is formed, as shown in Fig. 6. The formation process and mechanism of the bright layer are still under further investigation.

3.4. Corrosion in liquid aluminum

The immersion of the sample in pure aluminum melt at 750 °C for 240 h had done no damage to the surface layer which is still in perfect condition with no change in the thickness. In contrast, the uncoated steel sample has presented some corrosion perforation in 8 h, and dissolved completely into aluminum melt in 10 h.

4. Conclusions

(1) The thickness of the pure aluminum layer on the steel substrate is reduced with the increase in temperature and time in the initial hot dipping stage, and the thickness of the aluminum layer does not increase with time at given temperature when identical temperature and complete wetting occur between liquid aluminum and the substrate surface.

(2) The thickness of the Fe–Al intermetallic layer on the steel base is increased with the increase in hot dipping temperature and time. According to the experimental data and the mathematics model developed by the study, a maximum exists in the thickness of the Fe–Al intermetallic at certain dipping temperature.

(3) The top portion of the coated steel substrate is composed of a thin layer of α-Al_2O_3, followed by a thinner layer of $FeAl_3$, and then a much thicker one of Fe_2Al_5 on the steel base side.

(4) A carbon-rich zone in diffusion front is formed in aluminizing at 710 °C for 120 min, and the zone still exists after immerging in liquid aluminum at 750 °C for 240 h.

(5) The surface of aluminum oxide formed on the steel substrate is in perfect condition after corrosion test in liquid aluminum at 750 °C for 240 h, showing extremely good resistance to aluminum melt corrosion.

References

[1] G.A. Mollere, US patent 2315725 (1948).
[2] T. Sendzimir, US patent 2110893 (1938).
[3] G. Willam, Wood Metal Handbook, Surface Cleaning, Finishing and Coating, ninth ed., vol. 5, ASM, Ohio, 1982, p. 333.
[4] T.C. Simpson, Corrosion 49 (7) (1993) 550.
[5] B Thaddeus, Massalski, Binary Phase Diagrams, vol. 1, ASM International, 1990, p. 148.

[6] D. Liang, et al., Scripta Metall. Meter. 34 (10) (1997) 1513.
[7] Ni Zhijian, Ren Zhongyuan, Huang Diguang, J. Northwestern Inst. Arch. Eng. 14 (3) (1997) 42 (in Chinese).
[8] R. Asthana, Metall. Mater. Trans. 26A (1995) 1307.
[9] L. Yaohui, H. Zhenming, Y. Sirong, D. Guitian, L. Qingchun, J. Mater. Sci. Lett. 11 (1992) 896.
[10] Jiang Hanying, Physical Chemistry in Hydrometallurgy, Metallurgy Industry Publisher, Beijing, 1984 (in Chinese).
[11] T. Heumann, N. Dittrich, Z. Metallk 50 (1959) 617.
[12] Chen Jun, New Technol. Process (1) (1999) 26 (in Chinese).
[13] L.N. Larikov, V.M. Falchenko, D.F. Polishebuk, V.R. Ryabov, A.V. Lonovskays, in: G.V. Samsonov (Ed.), Protective Coatings on Metals, vol. III, Consultant Bureau, New York, 1971, p. 56.
[14] P.K. Rohatgi, C.S. Nath, Wang Deqing, in: P.K. Rohatgi (Ed.), Microstructure Formation During Solidification of Metal Matrix Composites, TMS Publication, 1993, p. 149.